Available online at www.sciencedirect.com

ScienceDirect

Ceramics International 40 (2014) 1359–1363

CERAMICS INTERNATIONAL

www.elsevier.com/locate/ceramint

Joining of silicon carbide and graphite by spark plasma sintering

Tomoyuki Okuni[a,b], Yoshinari Miyamoto[a,b,*], Hiroya Abe[b], Makio Naito[b]

[a]*Advanced Carbon Technology Center, Toyo Tanso Co., Ltd., 5-7-12 Takeshima, Nishiyodogawa-ku, Osaka 555-0011, Japan*
[b]*Joining and Welding Research Institute, Osaka University, 11-1 Mihogaoka, Ibaraki, Osaka 567-0047, Japan*

Received 18 March 2013; accepted 2 July 2013
Available online 8 July 2013

Abstract

After placing SiC powder on an isotropic graphite substrate, the two materials were successfully joined by spark plasma sintering (SPS). The effect of an Al_2O_3–Y_2O_3 sintering aid on SiC during joining was studied. The tensile strength of the joints prepared at 1800 °C under 30 MPa for 5 min reached 18 MPa. The fracture occurred not at the interface, but at the graphite substrate. The joining mechanism of SiC/graphite is attributed to the following: after the SiC powder squeezes into the open pores of graphite during sintering, the sintered SiC produces a strong bond through the interface between SiC and graphite.

Keywords: A. Joining; Graphite; Silicon carbide; Spark plasma sintering

1. Introduction

Isotropic graphite materials are typically produced using the following process: after mixing filler coke with binder pitch, the mixture is cold isostatically pressed, baked at about 1000 °C, and then graphitized at about 3000 °C by the Acheson method [1,2]. The combination of cold isostatic pressing and graphitization results in high quality graphite with isotropic properties that is easy to machine. Large graphite blocks ranging in size from several tens of centimeters to several meters can be produced. The blocks are machined into a variety of products used in various industries, including crucibles, molds, heaters, electrodes, heating trays, and others. The material's high refractoriness, excellent thermal shock and chemical resistance, appropriate electric and thermal conductivities, self-lubrication, and light weight make it suitable for these applications. However, one limitation is its low strength, which is a result of its high porosity (9–25%) [2,3]. This high porosity is caused by the low carbon yield of the binder pitch after baking.

In order to further expand the applications of graphite, it is joined to or coated with strong and hard ceramics or tough metals. Forming metal/graphite joints by using brazing metals [4–7], or by solid state bonding has been studied [8–14]. However, only a few investigations on joining of ceramic/graphite, using brazing metal [15] and adhesives [16] have been reported in the literature. Moreover, most ceramic/graphite joints are prepared below 1400 °C, which reduces the working temperature of the joints. Many brazing metals are limited to low-temperature applications because of their low melting points and mismatched coefficients of thermal expansion (CTE) with graphite. In addition, few studies on joining of ceramic and graphite for higher temperature applications exist in the open literature. By directly joining ceramics to graphite without requiring brazing metals or adhesives, high temperature applications are possible.

On the other hand, SiC-coated graphite susceptors prepared by CVD are widely used for the epitaxial growth of Si, GaN and other compound semiconductors in the electronic, lighting, and laser industries. The SiC coating protects the semiconductor crystals from being contaminated by the carbon particles and gas emissions from the susceptors and prevent corrosion of graphite with process gasses at high temperature. In this case, the coating is only several tens of microns in thickness. By forming a strong joint of thicker and denser SiC with graphite would further improve the graphite's resistance to hot corrosion and wear, as well as its toughness.

Spark plasma sintering (SPS) is an efficient process to sinter ceramics and metals [17–21]. It is also used for joining of

---

[*]Corresponding author at: Joining and Welding Research Institute, Osaka University, 11-1 Mihogaoka, Ibaraki, Osaka 567-0047, Japan.
Tel./fax: +81 6 6879 4373.
E-mail address: miyamoto@jwri.osaka-u.ac.jp (Y. Miyamoto).

0272-8842/$ - see front matter © 2013 Elsevier Ltd and Techna Group S.r.l. All rights reserved.
http://dx.doi.org/10.1016/j.ceramint.2013.07.017

dissimilar ceramics or metals, and ceramic-to-metal combinations. For example, Kondo et al. reported that stacked powders of TiN and apatite were sintered and simultaneously joined by SPS [22]. ZrB_2/SiC joints [23] have also been fabricated.

In this study, the direct joining of SiC to graphite was carried out using SiC powders containing a sintering aid of Al_2O_3–Y_2O_3 by SPS. The effect of sintering aid on joining was investigated by analyzing the interface structure and its composition. The bonding strength was evaluated by tensile testing, and the joining mechanism was proposed.

2. Experimental procedure

Isotropic graphite (IG-12, Toyotanso Co., Ltd.) was selected because it has a similar coefficient of thermal expansion (CTE) (4.7×10^{-6}/K) to that of SiC (4.3×10^{-6}/K). The tensile strength of the graphite substrate is 28 MPa [2]. The bulk density and porosity are 1.78 Mg/m^3 and 21%, respectively. α-SiC powder (SER-A06, Shinano Electric Refining Co., Ltd.), with an average particle size of 0.6 μm, was mixed with Y_2O_3 (RU-P, Shin-Etsu Chemical Co., Ltd.) and Al_2O_3 (TM-DAR, Taimei Chemicals Co., Ltd.) as the sintering aid at 3 and 6 mass%, respectively. SiC powder (1.8 g) with or without sintering aid was placed on the top and bottom of a graphite substrate (∅25 × 4 mm) in a graphite mold (inner diameter: ∅25 mm).The graphite sheets (PF-50, Toyotanso Co., Ltd.) were placed between the joint and a graphite punch. The sintering was carried out at temperatures of 1800–2000 °C for 5 min under a pressure of 30 MPa in vacuum by SPS (SPS-1050, Sumitomo Coal Mining Co., Ltd.). Graphite spacers and punches were placed between the electrode and the mold. The joining temperature was determined by focusing a pyrometer into a 1-mm diameter hole made through the side of the mold.

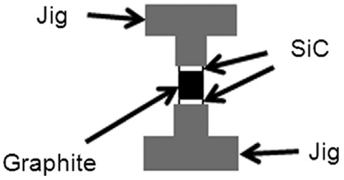

Fig. 1. Schematic of the jigs used for measuring the joining strength.

The sintered graphite/SiC joints were ground and polished to a size of ∅25 × 6 mm, and then cut into pieces of 4 mm (W) × 4 mm(L) × 6 mm(H) for microstructure observation and strength measurement. Microstructural observation and elemental analysis of the graphite/SiC joints were carried out by scanning electron microscopy – energy dispersive X-ray spectroscopy (SEM-EDS, ERA-8800FE, ELIONIX Co., LTD). Crystalline phases were examined by XRD (Ultima IV, Rigaku Corporation). The strength of the joints was measured by the tensile test (EZ-L, SHIMADZU CORPORATION). Fig. 1 shows a schematic drawing of jigs used for measuring the strength. The top and bottom of the joints were adhered to stainless steel jigs using an epoxy resin adhesive (E-60HP, Henkel AG & Co. KGaA) at 80 °C for about 24 h. The cross head speed of the tensile test was 0.5 mm/min. Seven test bars with the size of 4 mm(W) × 4 mm(L) × 6 mm (H) were prepared and subjected to tensile testing.

3. Results and discussion

Fig. 2 shows the interface structures of SiC/graphite joints. In the joints with sintering aid prepared at 1900 °C (Fig. 2a) and 2000 °C (Fig. 2b), graphite and SiC were tightly joined. No gaps and delaminations were observed. In contrast, in the joints without sintering aid prepared at 1900 °C (Fig. 2c) and 2000 °C (Fig. 2d), some gaps were observed at the interface. In addition, SiC ceramic parts without sintering aid had a

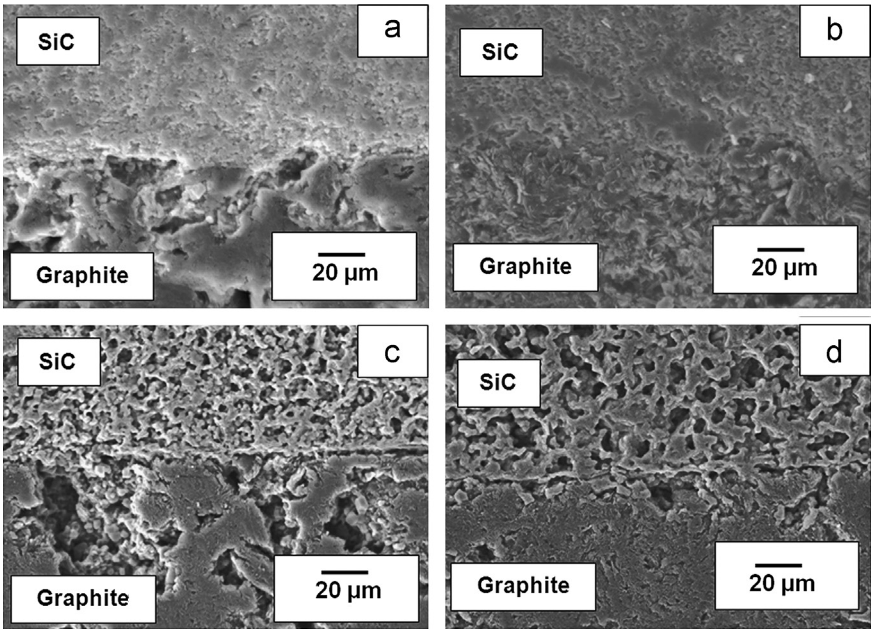

Fig. 2. Cross-sectional SEM images of SiC/graphite joints with sintering aid prepared at 1900 °C (a) and 2000 °C (b): without sintering aid prepared at 1900 °C (c) and (d) 2000 °C.

higher porosity. Many open pores were observed. These results suggest that the sintering aid contributes not only to the densification of SiC, but also to the joining of SiC with graphite.

Fig. 3 shows the cross-sectional images and elemental analysis of SiC/graphite joints with sintering aid. In the joint prepared at 1800 °C (Fig. 3a), Al, Y and Si elements were observed in the open pores of the graphite substrate, and their concentration looks similar to that in the top SiC layer. In the joint prepared at 1900 °C, similar results as that of the joint prepared at 1800 °C were observed, although they are not shown here.

However, in the joint prepared at 2000 °C as shown in Fig. 3b, a higher concentration of Al and Y elements in the graphite substrate were observed compared with that in the SiC layer. This result indicates a molten Si–Al–Y–O phase of low viscosity forms and penetrates into the open pores during sintering at 2000 °C.

According to the phase diagram of the system Y_2O_3–Al_2O_3–SiO_2, a liquid phase is formed during sintering even at 1500 °C [24]. The SiC layer with the sintering aid prepared at 1900 °C was denser than that with no sintering aid as shown Fig. 2(a) and (c).

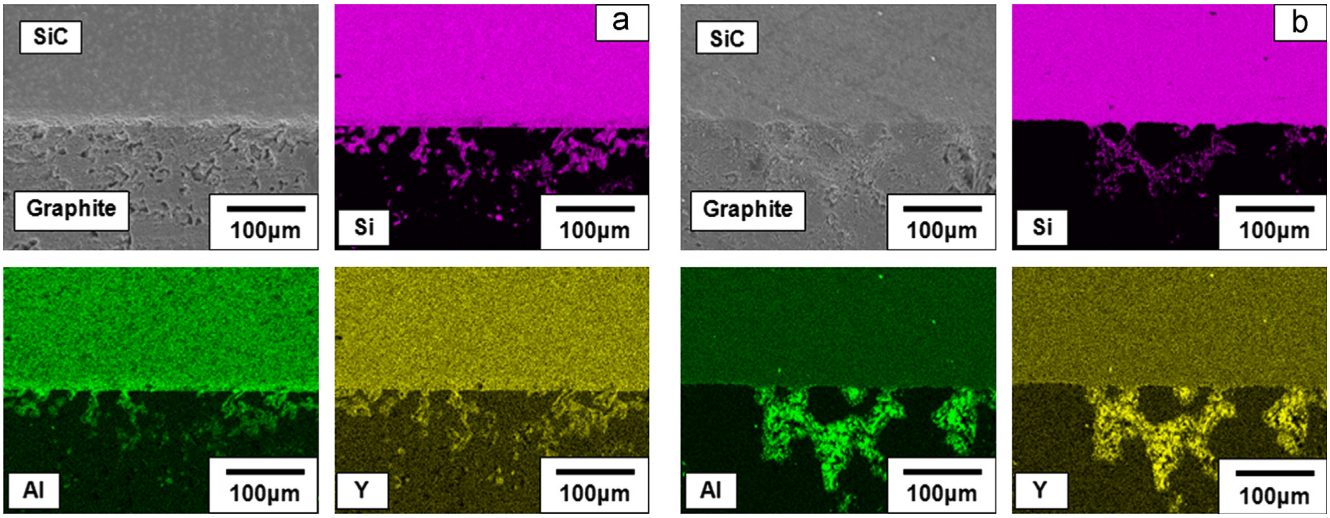

Fig. 3. Cross-sectional SEM images and elemental analyses of Si, Al, and Y at the interface of the SiC/graphite joints prepared with sintering aid at 1800 °C (a) and 2000 °C (b).

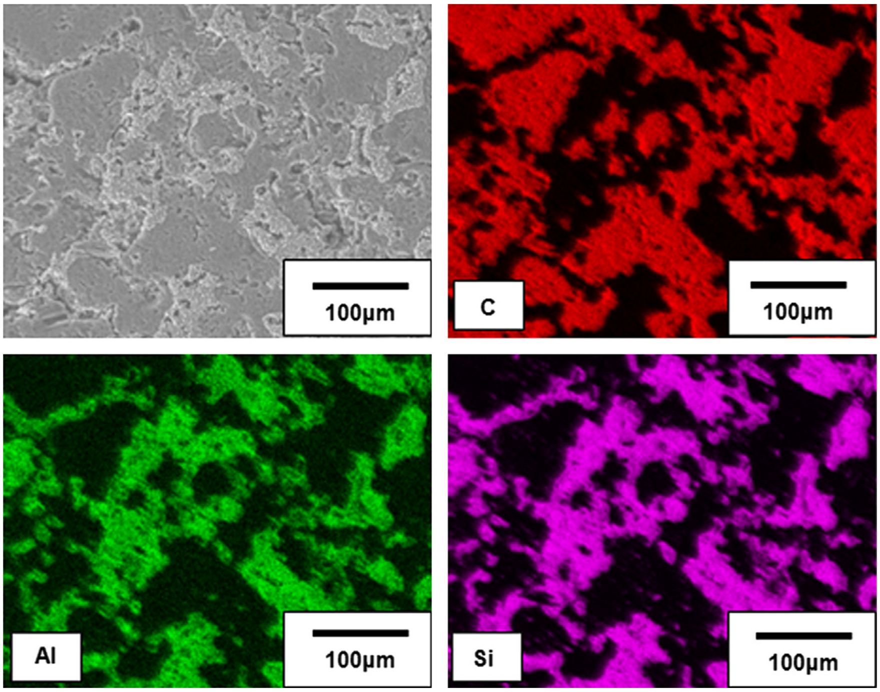

Fig. 4. SEM-EDS images of graphite side separated at interface sintered at 1800 °C. The sample was prepared by notching at the interface of a SiC/graphite joint and separating.

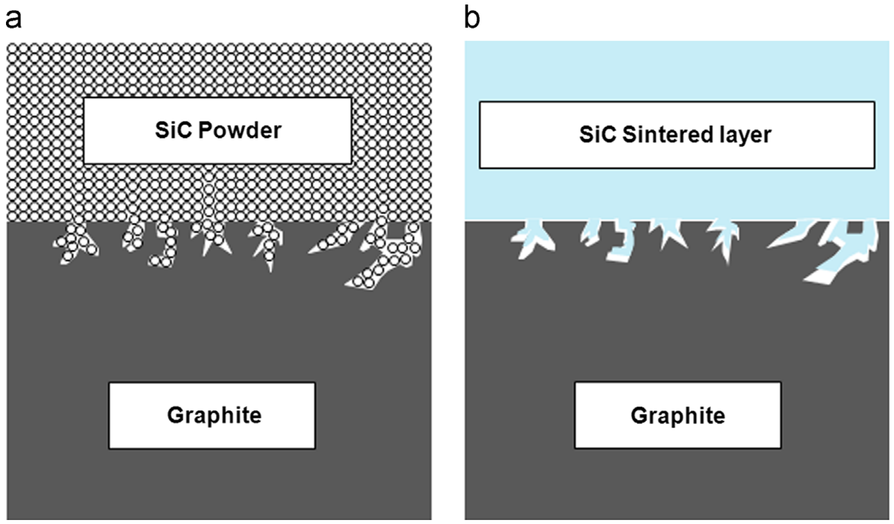

Fig. 5. Schematic of the joining mechanism between SiC and graphite (a) before sintering and (b) after sintering.

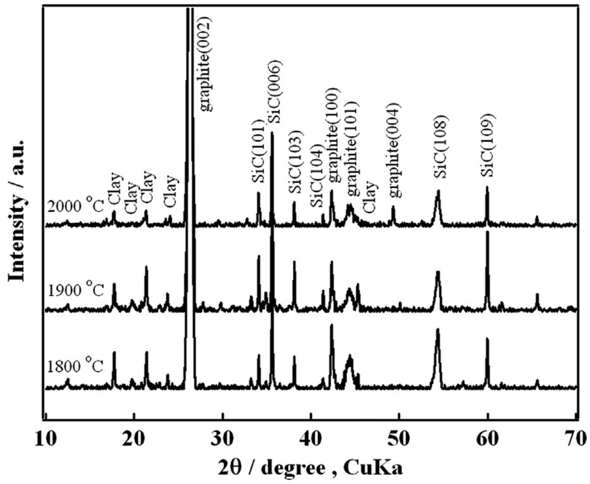

Fig. 6. XRD patterns of the SiC/graphite joints prepared at the temperature range of 1800 °C–2000 °C.

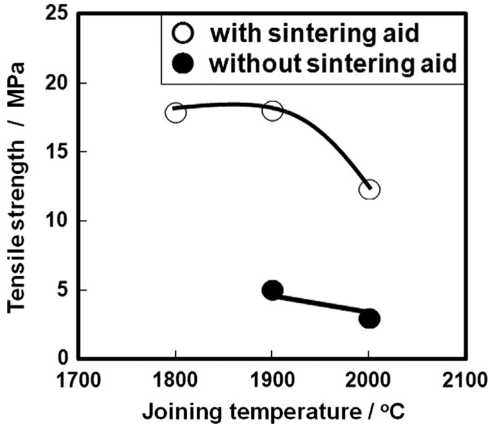

Fig. 7. Tensile strengths of SiC/graphite joints as a function of joining temperature with sintering aid (○) and without sintering aid (●).

Fig. 4 shows the graphite side separated at the interface when the joint was prepared at 1800 °C. The separation of the SiC/graphite joint was intrinsically made by notching at the interface. The contrast appearing between C and Si, Al elements indicates that a high concentration of SiC exists in the open pores of the graphite substrate. Because the graphite has high porosity, some of the SiC powders fill the pores and are sintered through the interface between SiC and graphite. The sintered SiC located in the pores of graphite acts as an anchor to the joint, as illustrated in Fig. 5.

Fig. 6 shows XRD patterns of the graphite/SiC joints. Diffraction peaks appearing at 18°, 21° and 25° are from the clay used to fix the XRD samples. Only α(6H)–SiC and graphite were detected and no crystalline phase of the Si–Al–Y–O system was identified even in the joints prepared at 2000 °C. The Si–Al–Y–O phase appears as a glass phase.

Fig. 7 shows the relationship between the joining temperature and the average strength of all graphite/SiC joints with and without sintering aid. Almost all of the joints with sintering aid fractured at the graphite substrate near the interface, while the joints without sintering aid fractured at the interface. Since the sample without the sintering aid showed very low strength of about 4 MPa, the sintering aid contributed to not only sintering, but also joining of graphite with SiC. At the temperature range of 1800 °C–1900 °C, the average strength of the joints with sintering aid reached 18 MPa. Since the fracture occurred at the graphite substrate, the true bonding strength at the interface of their joints would exceed 18 MPa. The residual stress may lead to strength degradation of the graphite substrate (18 MPa) from the original graphite (28 MPa). As a simple estimation, the thermal stress of graphite joined with SiC is calculated to be 8 MPa as a tensile stress mode by using the following:

$$\sigma = \Delta\alpha \Delta T E \tag{1}$$

where, σ is the thermal stress, $\Delta\alpha$ is the difference of linear coefficients of thermal expansion between SiC and graphite, E is the elastic modulus of graphite, and ΔT is the temperature difference between sintering and room temperature. The measured bonding strength of the joint, which represents the tensile strength of graphite near the joining interface, is 18 MPa. The strength degradation to 10 MPa compared to the original strength of graphite is the almost same as the calculated thermal stress (8 MPa). Therefore, the strength degradation should be caused by the thermal stress between graphite and SiC.

On the other hand, the strength of the joint prepared at 2000 °C decreased to 12 MPa. The fracture also occurred at the graphite substrate near the interface. Since the graphite and SiC were tightly joined by the sintered SiC grains at 1800 °C, the additional stress at the graphite substrate near the interface may be induced by squeezing the molten Al–Y–O phase into the graphite pores. The glass phase observed in the graphite substrate increases the elastic modulus and CTE of graphite near the interface.

4. Conclusions

Isotropic graphite and SiC were successfully joined by using SPS. No cracks or delaminations were observed at the graphite/SiC interface. The average tensile strength of the joints reached 18 MPa when joined at 1800 °C. The fracture occurred not at the interface, but at the graphite substrate. It indicates the bonding strength at the interface exceeding 18 MPa. A simple estimation of the thermal stress at the joint corresponded to the degradation of tensile strength of graphite from the original strength of 28 MPa to 18 MPa. The joining mechanism is attributed to the following: after the SiC powder squeezes into the open pores of graphite during sintering, the sintered SiC produces a strong bond through the interface between SiC and graphite. The Y_2O_3–Al_2O_3 sintering aid helps to densify SiC and join SiC to graphite. When joined at 2000 °C, the sintering aid melts into a low-viscosity glass phase and penetrates into the open pores of graphite. Because the glass phase has a high elastic modulus and CTE, it reduces the joining strength to 12 MPa. The joining method of SiC to graphite described here is simple and has potential for high temperature industrial applications.

References

[1] R.E. Nightingale, Nuclear Graphite, Academic Press, New York, 1962.

[2] Toyo Tanso Carbon Products Catalog. No. TSE-03-01, 2011, p. 6.

[3] T. Yamashina, T. Hino, Overall evaluation study for isotropic graphite as fusion first wall material in Japan, Journal of Nuclear Materials 162–164 (1989) 841–850.

[4] F. Brossa, E. Franconi, P. Schiller, Development of graphite/metals bondings for fusion reactor applications, Journal of Nuclear Materials 191–194 (1992) 469–472.

[5] Z. Zhou, Z. Zhong, J. Chen, C. Ge, The development of joining doped graphite to copper for first wall application in HT-7 tokamak, Fusion Engineering and Design 85 (2010) 1513–1516.

[6] S.S. Khirwadkar, K.P. Singh, Y. Patil, M.S. Khan, J.J.U. Buch, A. Patel, S. Tripathi, P.M. Jaman, L. Rangaraj, C. Divakar, Fabrication and characterization of tungsten and graphite based PFC for divertor target elements of ITER like tokamak application, Fusion Engineering and Design 86 (2011) 1736–1740.

[7] H. Ohmura, T. Yoshida, K. Kawamura, O. Yoshimoto, A technique for brazing graphite/graphite and stainless steel/high-carbon steel joints, Welding Research 73 (10) (1994) 249–256.

[8] H. Sueyoshi, T. Nishida, Solid state bonding of graphite to sus304 steel, Materials Transactions JIM 41 (3) (2000) 414–419.

[9] H. Sueyoshi, N. Fukuda, T. Nishida, Solid State Bonding of Graphite to S45C Steel, Materials Transactions JIM 39 (10) (1998) 1084–1092.

[10] H. Sueyoshi, T. Nishida, Solid state bonding of graphite to nickel, Materials Transactions 42 (1) (2001) 163–170.

[11] H. Sueyoshi, T. Nishida, Solid State bonding of graphite to inconel 718, Materials Transactions 42 (9) (2001) 1945–1951.

[12] T. Nishida, H. Sueyoshi, Effects of carbon fiber orientation and graphitization on solid state bonding of C/C composite to nickel, Materials Transactions 44 (1) (2003) 148–154.

[13] H. Sueyoshi, T. Nishida, Effects of joining compressive stress on solid state bonding of graphite to nickel, Materials Transactions 42 (12) (2001) 2559–2566.

[14] T. Nishida, H. Sueyoshi, Effect of graphitization on solid state bonding of carbon to nickel, Materials Transactions 47 (2) (2006) 399–404.

[15] J. Wang, N. Jiang, H. Jiang, The high-temperatures bonding of graphite/ceramics by organ resin matrix adhesive, International Journal of Adhesion and Adhesives 26 (2006) 532–536.

[16] Y. Mao, S. Li, L. Yan, Joining of SiC ceramic to graphite using Ni–Cr–SiC powders as filler, Materials Science and Engineering A 491 (2008) 304–308.

[17] P. Anger, L.G. Yu, K.A. Khor, G. Korb, I. Zalite, Spark-plasma-sintering (sps) of nanostructured titanium carbide powders, Journal of the European Ceramic Society 25 (2005) 1919–1927.

[18] L. Gao, J.S. Hong, H. Miyamoto, S.D.D.L. Torre, Bending strength and microstructure of Al_2O_3 ceramics densified by spark plasma sintering, Journal of the European Ceramic Society 20 (2000) 2149–2152.

[19] W. Li, L. Gao, Rapid sintering of nanocrystalline ZrO_2(3Y) by spark plasma sintering, Journal of the European Ceramic Society 20 (2000) 2441–2445.

[20] K.A. Khor, L.-G. Yu, S.H. Chan, X.J. Chen, Densification of plasma sprayed YSZ electrolytes by spark plasma sintering (SPS), Journal of the European Ceramic Society 23 (2003) 1855–1863.

[21] G. Xie, O. Ohashi, T. Yoshioka, M. Song, K. Mitsuishi, H. Yasuda, K. Furuya, T. Noda, Effect of interface behavior between particles on properties of pure Al powder compacts by spark plasma sintering, Materials Transactions 42 (9) (2001) 1846–1849.

[22] H. Kondo, A. Yokohama, M. Omori, A. Ohkubo, T. Hirai, F. Watari, M. Uo, T. Kawasaki, Fabrication of titanium nitride/apatite functionally graded implants by spark plasma sintering, Materials Transactions 45 (11) (2004) 3156–3162.

[23] W.R. Pinc, M.D. Prima, L.S. Walker, Z.N. Wing, E.L. Corral, Spark plasma joining of ZrB_2–SiC composites using zirconium–boron reactive filler layers, Journal of the American Ceramic Society 94 (11) (2011) 3825–3832.

[24] Y. Murakami, H. Yamamoto, Phase diagram of Al_2O_3–Y_2O_3–SiO_2 oxides system and its application to ceramics, Mitsubishi Juko Giho 28 (6) (1991) 552.